ASSESSMENT OF TRANSITION MODELS FOR AERODYNAMIC APPLICATIONS

Márcio Teixeira de Mendonça
Centro Técnico Aeroespacial
marcio_tm@yahoo.com

Paulo Vatavuk
Universidade de Campinas
pvatavuk@fec.unicamp.br

Abstract. *This paper presents comparisons of different boundary layer laminar-turbulent transition onset and transition length models implemented on a boundary layer code. The test cases are ¤at plate with zero pressure gradient and favorable and adverse pressure gradient cases and a test case for the boundary layer over a elliptic cylinder. Different turbulent levels are considered. The onset models are simple empirical correlation models and the transition length models are based on the intermittency factor. The results show that the transition length is reasonably captured by the models, but the onset models should be used with care and the resulting onset location considered as trends rather than precise results.*

Keywords: *transition to turbulence, boundary layers, turbulence intermittency, transition onset*

1. Introduction

A boundary layer developing over an airfoil is initially laminar close to the leading edge. Due to forced disturbances the boundary layer is led to a turbulent state. These disturbances may be related to velocity, pressure or temperature ¤uctuations and are known as rotational, acoustic and entropic modes. They may also be connected to wall vibration or wall roughness.

The skin friction coeff£cients for laminar and turbulent boundary layers are different by orders of magnitude. Therefore, airfoil design procedures must take into account boundary layer transition related to both the transition onset and the transition length. The estimation of transition onset and transition length is particularly important in low Reynolds number applications such as high lift devices and for the correct interpretation of wind tunnel results.

In the present paper an assessment of different transition length and onset models is performed. In Sec. 2 different test cases are used to evaluate the performance of the transition length model presented by Cebeci and Smith [Cebeci and Smith, 1974]. Section 3 presents a comparison of five transition onset models and five different intermittency models. Conclusions are presented in Sec. 4.

2. Transition Model Evaluation

This section presents the results for the evaluation of the transition length model suggested by Cebeci and Smith [Cebeci and Smith, 1974] and implemented in a boundary layer code. In order to evaluate the transition model, six test cases were chosen. The first three consider the ¤ow over ¤at plates with no pressure gradients, but with different turbulence levels in the free-stream (Baek e Chung [Baek and Chung, 2001]). The fourth test case considers the ¤ow around an elliptic cylinder (Schubauer [Schubauer, 1955]). The two last test cases consider the ¤ow over a ¤at plate with pressure gradient (Suzen and Huang [Suzen and Huang, 1999]).

The test cases 1, 2, 3, 5 and 6 are test cases of the Special Interest Group in Laminar-turbulent Transition (ercoftac.mech.surrey.ak.uk) of the "European Research Community on Flow, Turbulence And Combustion" (ERCOFTAC). These cases are called T3A, T3B, T3AM, T3C1 e T3C2 respectively.

2.1 Test Cases T3A, T3B, T3AM

The results presented in this section correspond to the results for the ¤ow over ¤at plates without pressure gradient. The test conditions for each case T3A, T3B, T3AM are respectively: $U_0 = 5.2, 9.4, 19.8$ (m/s); $L = 1.495, 1.495, 1.552$ (m); $T_u = 3.0, 6.0, 1.0$ (%); $X_{TR}/L = 0.25, 0.05, 0.85$. Where U_0 is the free-stream velocity, L is the plate length, T_u is the free-stream turbulence level and x_{TR} is the transition starting position.

Figure 1 presents the skin friction coeff£cient $C_f = (\mu \partial u/\partial y)/(0.5\rho U_0^2)$ versus local Reynolds number $Re = U_0 x/\nu$, for the three cases considered . A good agreement with the experimental and theoretical results can be observed. The streamwise position where transition starts was selected to give the best agreement with the experimental data, since the transition model available in the code does not predict the transition starting point. Suzen and Huang

[Suzen and Huang, 1999] give an estimate of the transition starting point slightly different than the ones chosen for the present results. This estimate is based on the experimental data, using as criterion the minimum skin friction. Nevertheless, the experimental data does not allow a great precision in the determination of minimum skin friction.

The transition region extent is predicted with good accuracy, despite the fact that the available model does not take into account the free-stream turbulence level. The free-stream turbulence changes both the transition starting position and the transition length. The model predicts a shorter transition region, not been able to capture the initial gradual departure from the laminar state observed experimentally.

The end of the transition region predicts an overshooting in the skin friction coef£cient. Further investigations has shown that this error is associated with the turbulence model implemented in the code and not to the intermittency model. The turbulence model implemented in the code considers a modi£ed Van Driest dumping function, which is made dependent on the momentum thickness Reynolds number. Changing the original turbulence model for the classic Cebeci and Smith [Cebeci and Smith, 1974] it was possible to arrive at better results for the region close to the end of the transition and beginning of the turbulent region, avoiding the overshooting.

2.2 Elliptic Cylinder

The next text case considers the experimental data from Schubauer [Schubauer, 1955] for the boundary layer on an elliptic cylinder. This test case tests the transition model with respect to favorable and adverse pressure gradients with a turbulent separation region. The elliptic cylinder has major and minor axes of 0.2992 m and 0.1011 m respectively. The far field velocity is 18.29 m/s. The non-dimensional pressure distribution around the elliptic cylinder is given in [Schubauer, 1955] in therms of $(p - p_s)/q$,

where p_s is the undisturbed stream static pressure and $q = .5\rho U_0$ is the undisturbed stream dynamic pressure. The Reynolds number based on the cylinder major axis is $Re = 364840$ and the free-stream turbulence is $T_u = 4.8\%$. Separation takes place at the streamwise position over the cylinder equal to $x = 0.2942$ m. The transition region extends from $x = 0.1264$ m to $x = 0.2295$ m. The streamwise extent of the elliptic cylinder surface is $x_L = 0.3339$ m

Figure 2 shows the skin friction variation along the surface of the cylinder. The transition starting position was imposed at the same streamwise position reported by Schubauer. The results are in reasonable agreement with the experimental results. Considering the scatter of experimental points, the length of the transition region was captured by the model with good accuracy. The turbulent skin friction is well predicted, even close to the separation point. The separation region predicted by the boundary layer code is in good agreement with the experimental observation.

Schubauer also report streamwise velocity pro£les at different streamwise positions. The velocity pro£les are compared with numerical results in Figure 3. Good comparisons are obtained for the laminar, transitional and turbulent velocity pro£les. In the region of strong adverse pressure gradient and close to the separation point, the predictions are slightly off.

In summary, regarding the transition region, the model was able to capture with good accuracy the transition length and the skin friction variation.

2.3 Test Cases T3C1 and T3C2

Test cases T3C1 and T3C2 correspond to the ¤ow over ¤at plates with variable pressure gradient that starts favorable in the beginning of the plate and becomes adverse in the end region of the plate. The test conditions for each case T3C1 and T3c2 are respectively $U_0 = 5.9, 5.0$ (m/s); $L = 1.495, 1.495$ (m); $T_u = 6.6, 3.0$ (%); $X_{TR}/L = 0.13, 0.53$.

Figure 4 presents the skin friction coefficient versus the dimensionless coordinate, x/C (C -length of the plate), for case T3C1. The results are presented for the classic Cebeci and Smith turbulence model and a similar model with a modified Van Driest dumping function, which is made dependent on the momentum thickness Reynolds number. The modified model is the one originally implemented in the boundary layer code. It can be noticed that the original model predicts a higher skin friction than the experimental values and the Cebeci-Smith model predicts lower values. These results are consistent with the previous zero gradient results, where the original model presented an overshoot in the skin friction values, but here the modified model showed a better agreement with the experimental values in the end region of the plate.

The transition is taken into account in the boundary layer model by the intermittency factor. This factor is the same in both turbulence models. So the transition length is the same in both versions. The results near x/c=0,3 may be and indication that the calculated intermittency is increasing faster than the experimental values.

Figure 5 presents the velocity profiles for case T3C1. The numerical results are indicated by a solid line and were obtained with the classic Cebeci and Smith model. It can be noticed that the agreement between the velocity profiles is very good, although the agreement between the skin frictions was not so good. The results obtained with the original turbulence model were very close to ones of the classical model and are not presented.

In figure 6 the skin friction for case T3C2 is presented. In this set of results the transition is starting much further downstream than in the previous set of results. This is due to the Reynolds number reduction of about 20% and mostly because of the turbulence intensity outside the boundary layer, which is reduced from 6% to 3%. It can be noticed that

also in this case the original turbulence model presented a better agreement with the experimental values in the end region of the plate. In these results also, the calculated intermittency seems to be increasing faster than the experimental values just after the beginning of transition, resulting in higher predicted Cf values around x/C=0,65.

In £gure 7 the velocity pro£les for case T3C2 are presented. In these results also a close agreement with the experimental values were obtained. It seems that the velocity pro£les are not so sensitive to imperfections in the model as the skin friction.

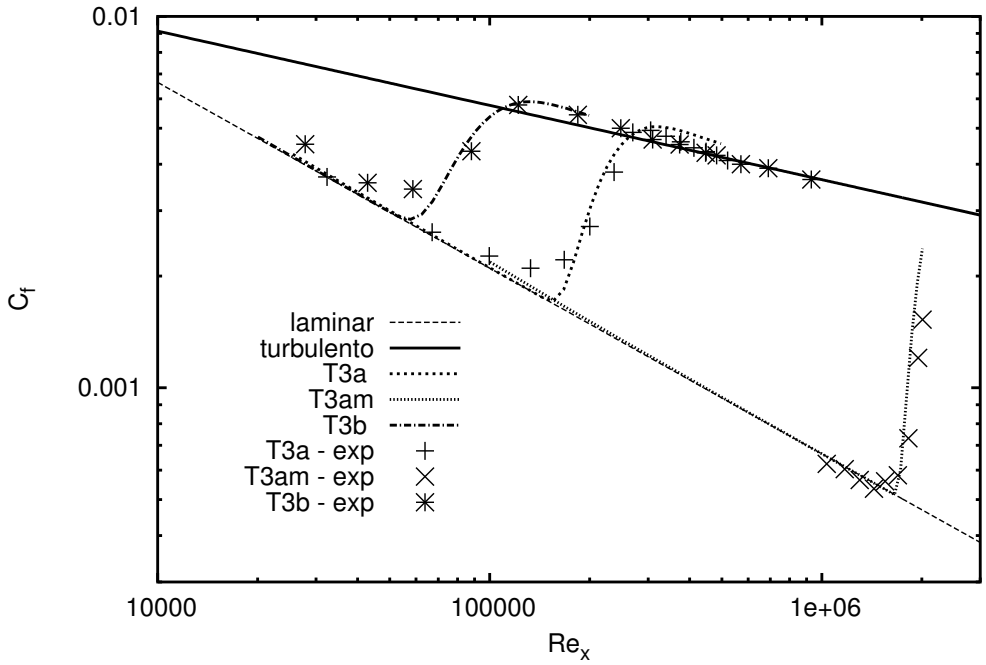

Figure 1: Skin friction coefficient along the plate. Test cases T3A, T3B and T3AM. Original turbulence model.

3. Alternative Transition Models

This section presents the test results for five transition onset correlations and the five intermittency correlations that have been implemented in the boundary layer code. The onset position computed with the different models are compared to the experimentally observed transition onset for six different test cases. The intermittency correlations are evaluated by comparing the skin friction distribution results obtained with each one for two variable pressure gradient test cases.

3.1 Transition Onset Models

Five different transition onset prediction models were implemented. They provide an estimated value for the streamwise position where the transition starts. Out of the five correlations the ones that are theoretically the more appropriate for aeronautical applications are by Dey and Narasimha [Dey and Narasimha, 1990] and Govindarajan and Narasimha [Govindarajan and Narasimha, 1991], where the free-stream turbulent intensity is usually low. The correlations by Abu-Ghannam and Shaw [Abu-Ghannam and Shaw, 1980], Mayle [Mayle, 1991] and the correlation by Suzen and Huang [Suzen and Huang, 1999] are more appropriate for applications with a high free-stream turbulent intensity, which would result in by-pass transition. The five correlations are presented below.

3.1.1 Abu-Ghannam & Shaw [Abu-Ghannam and Shaw, 1980]

Transition starts when the momentum thickness Reynolds number Re_θ is greater than:

$$Re_{\theta tr} = 163 + \exp\left[F(\lambda_\theta)\left(1 - \frac{Tu}{6.91}\right)\right]. \tag{1}$$

Where $\lambda_\theta = (\theta^2/\nu)dU_e/dx$, θ is the momentum thickness, ν is dynamic viscosity, dU_e/dx is the freestream velocity gradient and

$$F(\lambda_\theta) = 6.91 + 12.75\lambda_\theta + 63.64\lambda_\theta^2 \quad \lambda_\theta \leq 0, \text{ or } F(\lambda_\theta) = 6.91 + 2.48\lambda_\theta - 12.27\lambda_\theta^2 \quad \lambda_\theta > 0. \tag{2}$$

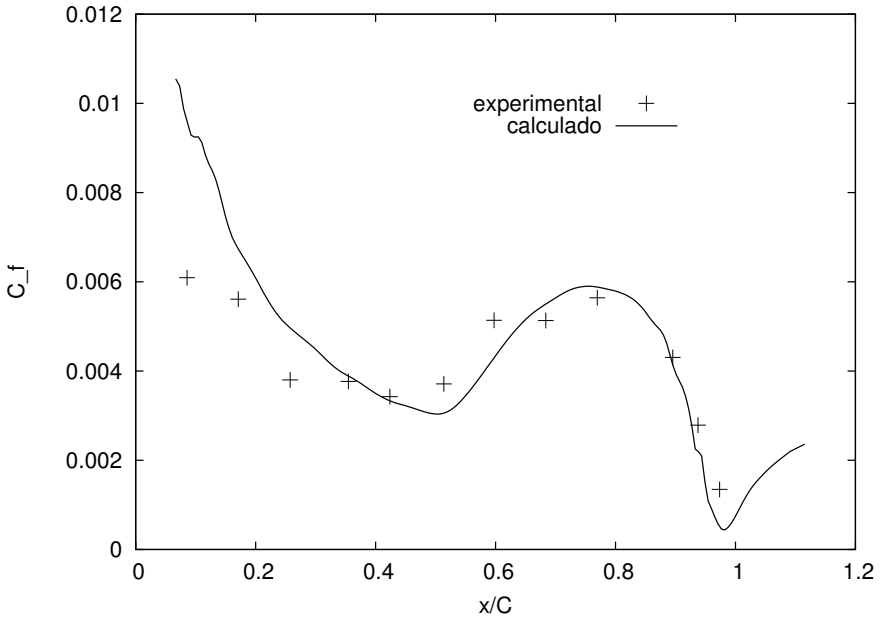

Figure 2: Skin friction along the surface of an elliptic cylinder.

3.1.2 Suzen & Huang [Suzen and Huang, 1999]

Transition starts when the momentum thickness Reynolds number is greater than:

$$Re_{\theta tr} = (120 + 150Tu^{-2/3})\coth\left[4(0.3 - K_t \times 10^5)\right]. \tag{3}$$

Where K_t is the maximum absolute value of the acceleration parameter $K = \frac{\nu}{U_e^2}\frac{dU_e}{dx}$ and Tu the freestream turbulence intensity in %.

3.1.3 Govindarajan & Narasimha [Govindarajan and Narasimha, 1991]

The momentum thickness Reynolds number is correlated to the onset position by:

$$Re_{\theta tr} = Re_{\theta tr0}\left[1 + 0.17\mathrm{e}^{-(Tu^2+Tu_0^2)}\frac{1-\mathrm{e}^{-60\lambda}}{1+0.4\mathrm{e}^{-60\lambda}}\right], \tag{4}$$

$$\lambda = (\theta^2/\nu)dU_e/dx \qquad Re_{\theta tr0} = 100 + 340/(Tu^2 + Tu_0^2)^{1/2}). \tag{5}$$

Where Tu_0 depends on the residual free-stream turbulence of each specific wind tunnel. On average one can assume $Tu_0 = 0.3$.

3.1.4 Dey & Narasimha [Dey and Narasimha, 1990]

The momentum thickness Reynolds number is correlated to the onset position by:

$$Re_{\theta tr} = 0.9Re_{\theta tr0}\left[1 + 0.15(\mathrm{e}^{-Tu} + 2)(1 - \mathrm{e}^{-60\lambda})\right], \tag{6}$$

$$Re_{\theta tr0} = 100 + 310/(Tu^2 + Tu_0^2)^{1/2}. \tag{7}$$

Where Tu_0 depends on the residual free-stream turbulence of each specific wind tunnel. On average one can assume $Tu_0 = 0.3$.

3.1.5 Mayle [Mayle, 1991]

Transition starts when the momentum thickness Reynolds number is greater than:

$$Re_{\theta tr} = 420.Tu^{-0.69}. \tag{8}$$

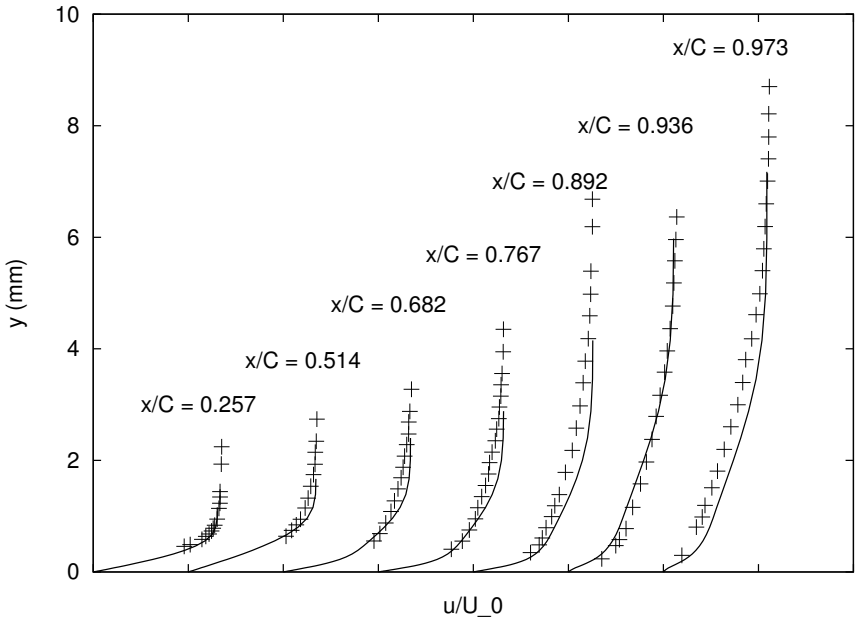

Figure 3: velocity distribution in the boundary layer along a elliptic cylinder.

Table 1: Transition onset prediction

	T3A	T3B	T3AM	Cylinder	T3C1	T3C2
Tu %	2.5	5.6	0.7	3.4	4.0	2.0
Abu-Ghannam	0.27	0.07	0.49	0.24	0.12	0.40
Suzen	0.26	0.10	0.16	0.29	0.13	0.24
Dey	0.18	0.05	0.23	0.26	0.13	0.37
Govindarajan	0.27	0.07	0.35	0.27	0.13	0.33
Mayle	0.23	0.04	0.32	0.23	0.10	0.29
Experiment	0.26	0.05	0.85	0.41	0.13	0.56

3.2 Transition Onset Results

The same six test cases presented in Sec. 2 are used to test the transition onset models. Table 1 presents the computed onset position for all five models and the observed transition position. Also indicated are the turbulence intensity Tu used in the computation, which correspond to the turbulence intensity at the onset position. The results show that all models perform similarly, but the model by Dey and Narasimha tend to estimate an earlier transition. None of the models performed well for the low free-stream turbulent intensity test case (T3AM). These models be used with care. preferably for ¤ows with turbulence intensity higher than 1%. For wing applications a much better onset prediction could be obtained with the e^N [Mendonça, 2000] method, which has not been implemented in this work.

3.3 Intermittency Models

Five different intermittency models have been implemented and tested. The £rst one from Arnal [Singer, 1993], the second from Narasimha [Stock and Haase, 2000], the third from Stock e Haase [Stock and Haase, 2000], and the last two from Chen and Thyson [Stock and Haase, 2000] and Abu-Ghannam and Shaw [Abu-Ghannam and Shaw, 1980]. The models by Arnal and by Narasimha are theoretically the most adequate for low free-stream turbulence intensity. The other models are applicable, but were originally developed for by-pass transition.

3.3.1 Arnal

The variable γ in this case is not exactly the intermittency factor defined by the turbulent spot formation theory of Emmons ([Narasimha, 1985], but a transition function.

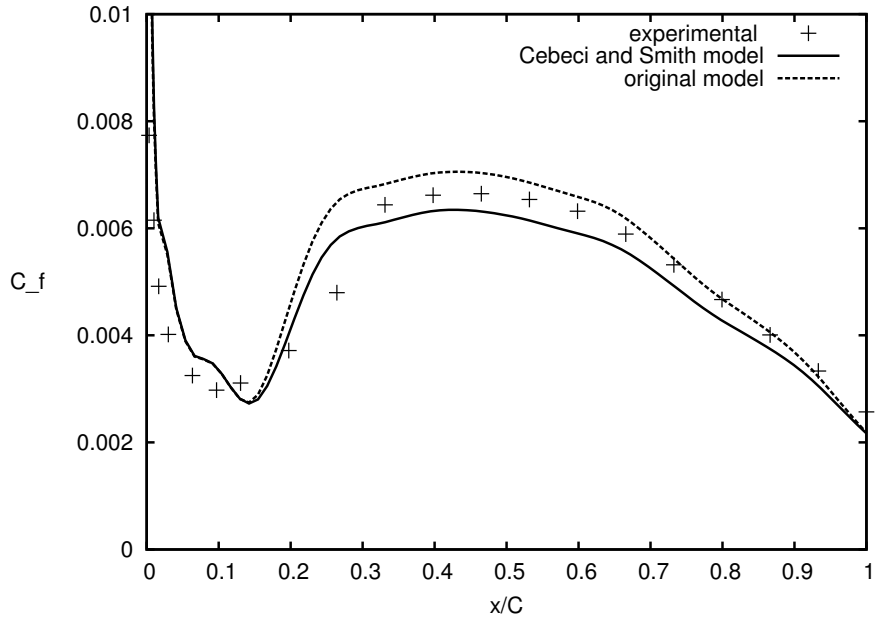

Figure 4: Skin friction coefficient for test case T3C1.

The transition function is governed by the parameter:

$$\chi = \frac{\theta/\theta_{t0} - 1. + 0.005Ma^2}{1 + .02Ma^2}. \tag{9}$$

Where Ma is the free-stream Mach number, θ is the local momentum thickness and θ_{t0} is the momentum thickness at the transition onset.

The transition function is computed by the following relations:

$$0 < \chi \leq 0.25, \qquad \gamma = 1 - \exp\left\{-4.5\left[\chi\left(1 + .02Ma^2\right) - 0.005Ma^2\right]^2\right\}, \tag{10}$$

$$0.25 < \chi \leq 0.75, \qquad \gamma = 18.628\chi^4 - 55.388\chi^3 + 52.369\chi^2 - 16.501\chi + 1.893, \tag{11}$$

$$0.75 < \chi \leq 3, \qquad \gamma = 1.25 - 0.25\sin\left[\pi\left(0.444\chi - 0.833\right)\right], \tag{12}$$

$$\chi > 3, \qquad \gamma = 1. \tag{13}$$

3.3.2 Narasimha

This is originally a linear combination transition region model, which considers that all ¤ow properties should be weighted by the intermittency factor. In the present implementation the intermittency factor is used as a transition function such that the effective viscosity μ_{eff} is given by:

$$\mu_{eff} = \mu + \gamma\mu_t. \tag{14}$$

In practice, many investigators use the intermittency factor as the transition function, and the same will be done in this work.

The universal turbulent intermittency function proposed by Dhawan and Narasimha [Dhawan and Narasimha, 1958] is given by:

$$\gamma = 1 - \exp\left(-0.411\xi^2\right). \tag{15}$$

Where:

$$\xi = (x - x_{tr})/\lambda, \quad x_{tr} = x_{\gamma=0} \quad (\text{xonset}), \quad \lambda = \Delta x/3.36. \tag{16}$$

Where Δx is computed from the empirical relation:

$$Re_{\Delta x} = 13.4Re_{\delta^*_{tr}}^{3/2}. \tag{17}$$

Where $Re_{\delta^*_{tr}}$ is the displacement thickness Reynolds number.

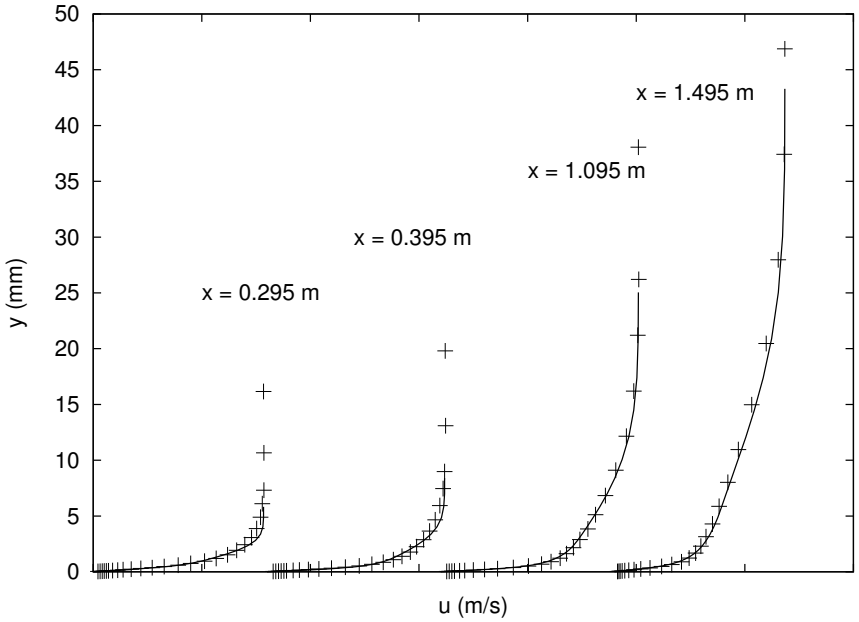

Figure 5: Velocity profiles for test case T3C1.

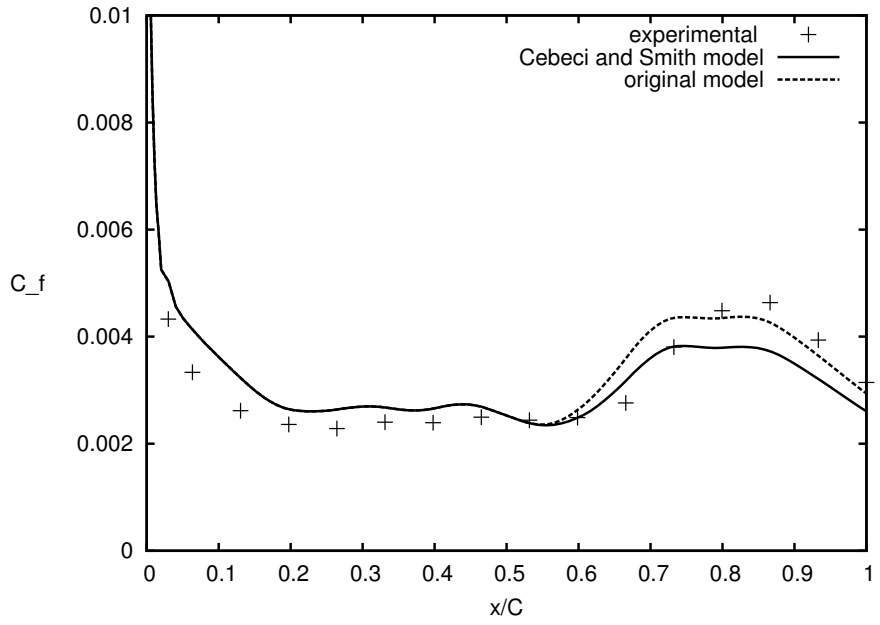

Figure 6: Skin friction coefficient for test case T3C2.

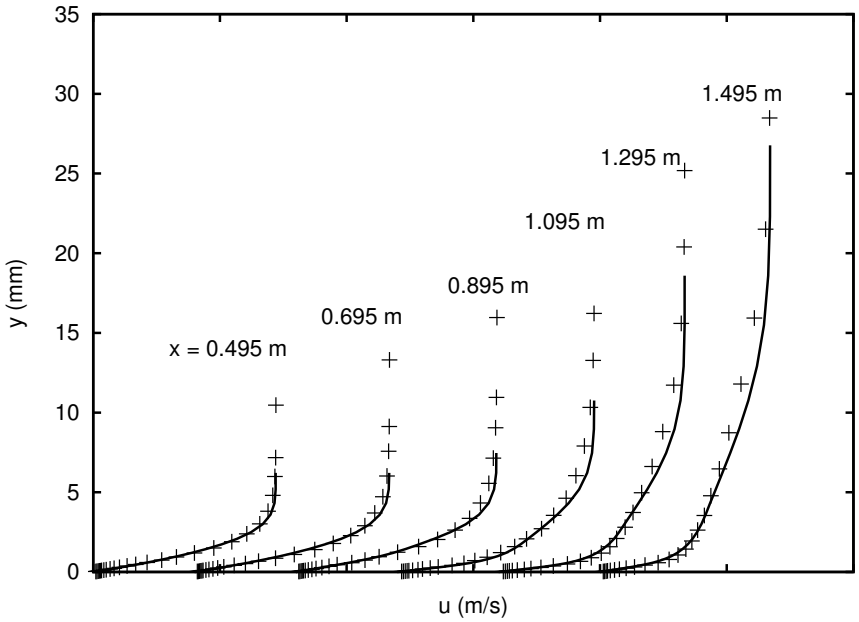

Figure 7: Velocity profiles for test case T3C2.

3.3.3 Stock and Haase

Stock and Haase proposed a model for the transition length to be used with the Narasimha intermittency function. It is given by:

$$Re_{\Delta x} = 4.6 Re_{\delta^*_{tr}}^{3/2}. \tag{18}$$

3.3.4 Chen and Thyson

Using the same intermittency function, Chen and Thyson proposed a transition length model that takes into account the effect of compressibility. The correlation is given by:

$$Re_{\Delta x} = (110.9 + 8.65 Ma^{1.92}) Re_{\delta^*_{tr}}^{4/3}. \tag{19}$$

3.3.5 Abu-Ghannam and Shaw

The transition function is given by:

$$\gamma = 1 - \exp\left(-5\eta^3\right), \tag{20}$$

for $Re_{\theta s} \leq Re_\theta < Re_{\theta e}$, where $Re_{\theta s}$ is the Reynolds number based on the momentum thickness at the start of the transition region, and $Re_{\theta e}$ is the momentum thickness Reynolds number at the end of the transition region. The value of $Re_{\theta s}$ is the onset value given by Eq. 1, or by a specified value. The end of the transition Region is related to the $Re_{\theta s}$ by $Re_{\theta e} = 2.667\ Re_{\theta s}$.

The parameter η is given by:

$$\eta = \left(\frac{Re_\theta - Re_{\theta s}}{Re_{\theta e} - Re_{\theta s}} \right)^{1/1.35}. \tag{21}$$

3.4 Intermittency Results

Two test cases were chosen to evaluate the performance of the five intermittency models implemented, the Schubauer elliptic cylinder and the ERCOFTAC test case T3C2. The results are presented in Figures 8 and 9. In all test cases the transition onset was specified equal to the experimentally observed values.

On both test cases the correlation by Arnal strongly overestimate the skin friction coefficient, with a short transition region. Arnal's model is tunned to vary between 0 and 1 at the start and end of the transition region. But in order to capture the overshooting of C_f at the end of the transition region observed in certain wing configurations tested by the developers of this correlation, it is allowed to reach a maximum value of 1.5. This may be the cause of the overshooting in the present

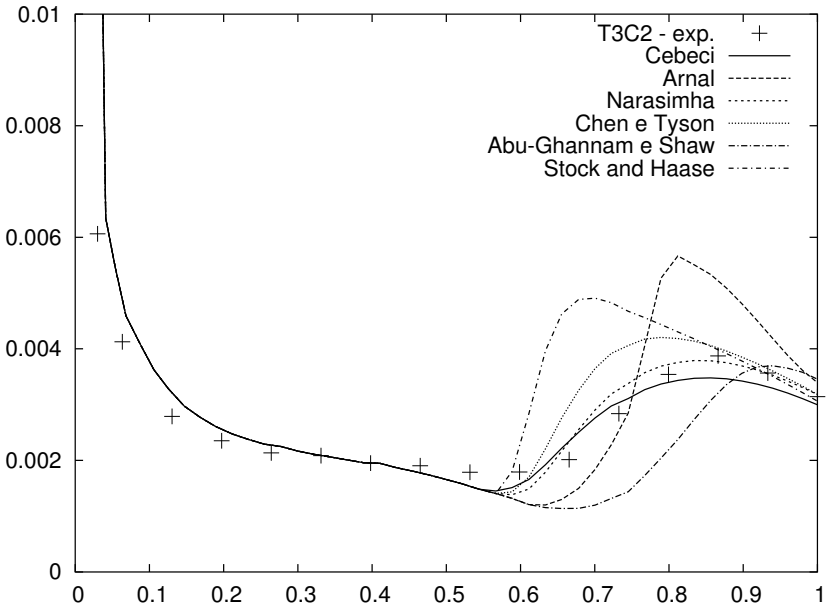

Figure 8: Friction coefficient distribution for test case T3C2 [Suzen and Huang, 1999].

test cases, since the model was not calibrated for the given turbulent intensities or pressure gradient distribution. The Stock and Haase's correlation also present a very short transition with a strong overshooting in the predicted C_f.

The correlations by Narasimha and Chen and Tyson performed relatively well for the T3C2 test case, with a better agreement for the Narasimha correlation.

For the ¤ow around the elliptic cylinder the same trends are observed. The best results are obtained with the Narasimha correlation. Comparing the results of all the new correlations with that of the original Cebeci and Smith transition model indicates no advantage in changing from Cebeci to any of the new correlations.

4. Conclusions

The transition model proposed by Cebeci and Smith [Cebeci and Smith, 1974] is able to predict the transition region with good accuracy, but in all ¤at plate test cases the transition region was shorter than the experimental observation.

Five transition onset correlations and five intermittency correlations were introduced in the boundary layer code and compared with experimental results and results from the original Cebeci and Smith correlation. The results show that, as long as the test cases presented are considered, the original correlation by Cebeci and Smith implemented in the boundary layer code gives the best results.

Regarding the transition onset, very good results were obtained for some of the test cases. But error as large as 100% were observed on other test cases. This correlations should be used with care and understood as trends in transition onset rather than precise values.

5. Acknowledgments

The authors would like to acknowledge the financial support provided by Embraer and FAPESP (grant 00/13768-4).

6. References

Abu-Ghannam, B. J. and Shaw, R., 1980, Natural transition of boundary layer-the effect of turbulence, pressure gradient and ¤ow history, "J. Mechanical Engineering Sciences", Vol. **22**, No. 5, pp. 213–228.

Baek, S. G. and Chung, M. K., 2001, k/ϵ model for predicting transitional boundary layer ¤ows under zero-pressure gradient, "AIAA Journal", Vol. **39**, No. 9, pp. 1699–1705.

Cebeci, T. and Smith, A. M. O., 1974, "Analysis of Turbulent Boundary Layers", Applied Mathematics and Mechanics—vol. 15, Academic Press.

Dey, J. and Narasimha, R., 1990, Integral method for the calculation of incompressible two-dimensional transitional boundary layer, "Journal of Aircraft", Vol. **27**, No. 10, pp. 859–865.

Dhawan, S. and Narasimha, R., 1958, Some properties of boundary layer ¤ow during the transition from laminar to turbulent motion, "Journal of Fluid Mechanics", Vol. **3**, pp. 418–436.

Govindarajan, R. and Narasimha, R., 1991, The role of residual non-turbulent disturbances on transition onset in two-

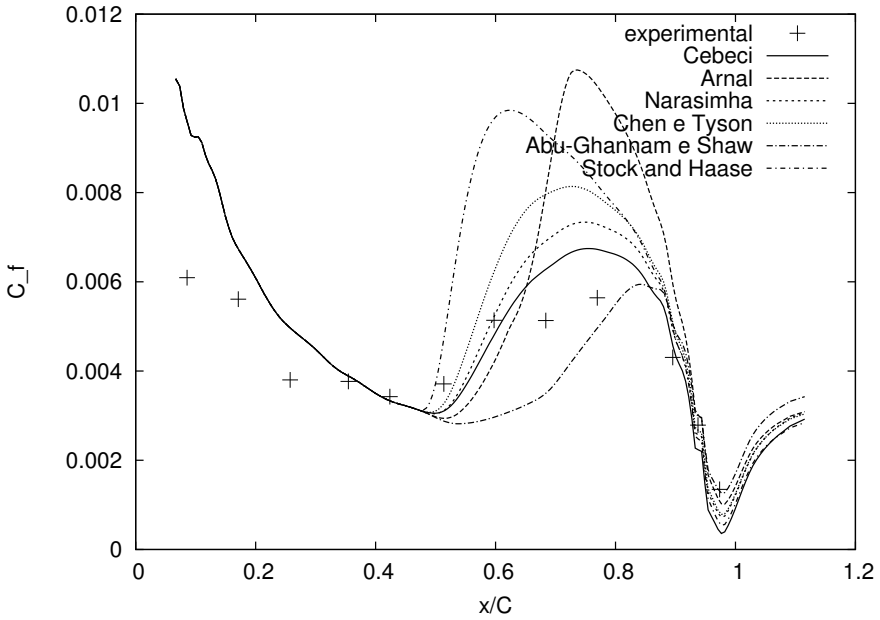

Figure 9: Friction coefficient distribution for the ¤ow around an elliptic cylinder [Schubauer, 1955].

dimensional boundary layers, “J. FLuids Eng.”, Vol. **113**, pp. 147–149.

Mayle, R. E., 1991, The Role of Laminar-Turbulent Transition in Gas Turbine engines, “J. Turbomachinery”, Vol. **113**, pp. 509–537.

Mendonça, M. T., 2000, “Laminar Flow Stability: Linear Theory”, chapter 5, pp. 98–147, Brazilian School of Transition and Turbulence. ABCM.

Narasimha, R., 1985, The Laminar-Turbulent Transition Zone in the Boundary Layer, “Prog. Aerospace Sci.”, Vol. **22**, pp. 29–80.

Schubauer, G. B., 1955, Air Flow in the boundary layer of an elliptric cylinder, Technical Report NACA 652, National Aeronautics and Space Administration – NASA.

Singer, B. A., 1993, Modeling the Transition Region, Technical Report NASA CR 4492, National Aeronautics and Space Administration – NASA.

Stock, H. W. and Haase, W., 2000, Navier-Stokes computations with e^N transition prediction including transitional ¤ow regions, “AIAA Journal”, Vol. **38**, No. 11, pp. 2059–2066.

Suzen, Y. B. and Huang, P. G., 1999, Modeling of ¤ow Transition using an intermittency transport equation, Technical Report NASA CR–1999-209313, National Aeronautics and Space Administration – NASA.

7. Responsibility notice

The author(s) is (are) the only responsible for the printed material included in this paper